# Identification of Multiple Structurally Distinct, Nonpeptidic Small Molecule Inhibitors of Protein Arginine Deiminase 3 Using a Substrate-Based Fragment Method

Haya Jamali, Hasan A. Khan, Joseph R. Stringer,[†] Somenath Chowdhury,[‡] and Jonathan A. Ellman*

Department of Chemistry, Yale University, New Haven, Connecticut 06520, United States

S Supporting Information

ABSTRACT: The protein arginine deiminases (PADs) are a family of enzymes that catalyze the post-translational hydrolytic deimination of arginine residues. Four different enzymologically active PAD subtypes have been characterized and exhibit tissue-specific expression and association with a number of different diseases. In this Article we describe the development of an approach for the reliable discovery of low molecular weight, nonpeptidic fragment substrates of the PADs that then can be optimized and converted to mechanism-based irreversible PAD inhibitors. The approach is demonstrated by the development of potent and selective inhibitors of PAD3, a PAD subtype implicated in the neurodegenerative response to spinal cord injury. Multiple structurally distinct inhibitors were identified with the most potent inhibitors having >10,000 min^{-1} M^{-1} k_{inact}/K_I values and ≥10-fold selectivity for PAD3 over PADs 1, 2, and 4.
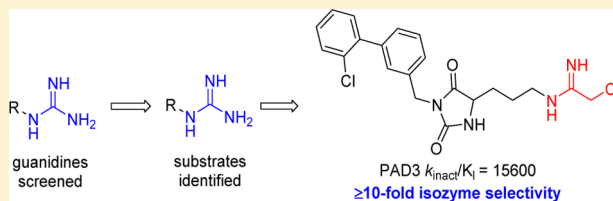
INTRODUCTION

The protein arginine deiminases (PADs) are a family of enzymes that catalyze the post-translational hydrolytic deimination of arginine residues (Figure 1A).[1−3] Several functionally
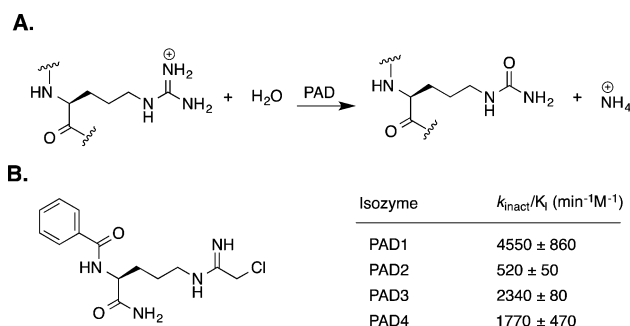

Figure 1. (A) Transformation catalyzed by PADs. (B) Cl-amidine, one of the most advanced PAD inhibitors.[16]

Isozyme	k_{inact}/K_I (min^{-1}M^{-1})
PAD1	4550 ± 860
PAD2	520 ± 50
PAD3	2340 ± 80
PAD4	1770 ± 470

active PAD subtypes, PAD1−4, have been characterized,[4−7] and though the primary structure of mammalian PADs is highly conserved, the human isozymes exhibit tissue-specific expression patterns.[3] Dysregulated PAD activity has been associated with multiple human diseases, including PAD1 for psoriasis,[8] PAD2 for multiple sclerosis,[9−12] and PAD4 for autoimmune disorders[13] and certain cancers.[14] Additionally, PAD3 has been implicated in the neurodegenerative response to spinal cord injury.[15]

The irreversible inhibitor Cl-amidine (Figure 1B) represents one of the most advanced PAD inhibitors.[5,16,17] Due to its low molecular weight, reasonably hydrophobic character, and nonpeptidic structure, Cl-amidine has shown activity in animal models[18] and has contributed to an improved understanding of the role of PADs in different diseases. However, Cl-amidine shows modest isozyme selectivity, with greatest potency against PAD1 and only poor activity against PAD2 and PAD3.[19,20] The lack of selectivity and moderate potency of Cl-amidine complicates deciphering the pharmacology of targeting the different isozymes. While more potent and selective larger peptidic inhibitors of PADs have been identified,[21−23] their activity in cells and animals has not been reported, and their peptidic nature poses challenges for proteolytic stability, cell permeability, and rates of metabolic clearance. The identification of low molecular weight, nonpeptidic, and isozyme-selective PAD inhibitors should facilitate a more thorough understanding of the individual roles of each PAD isozyme.

We have previously reported on a fragment-based approach for the discovery of enzyme inhibitors termed substrate activity screening (SAS).[24] The SAS method consists of the identification of nonpeptidic substrate fragments,[25] substrate optimization, and conversion of optimized substrates to inhibitors. The key advantage of this substrate-fragment discovery approach is that substrate hits are only identified upon productive binding and processing by the enzyme catalytic machinery. This approach minimizes undesirable false positives commonly observed in inhibitor screens, such as those due to small molecule micelle formation[26,27] or the presence of trace reactive impurities. The comparative ease of synthesis and assay of substrates relative to inhibitors is an additional advantage. We have successfully used this approach

for the identification of selective low molecular weight inhibitors of therapeutically relevant proteases[28−33] and phosphatases,[34−36] and other laboratories have implemented related strategies to target kinases.[37,38]

Herein, we report on the development of the SAS method for the identification of low molecular weight, nonpeptidic substrates, and inhibitors of PADs. Moreover, we report on the identification of multiple structurally distinct and selective small molecule inhibitors of PAD3, for which potent and selective compounds have not previously been reported.[20]

■ RESULTS AND DISCUSSION

The SAS method for the development of PAD inhibitors consists of three steps (Scheme 1): (1) a library of diverse, low

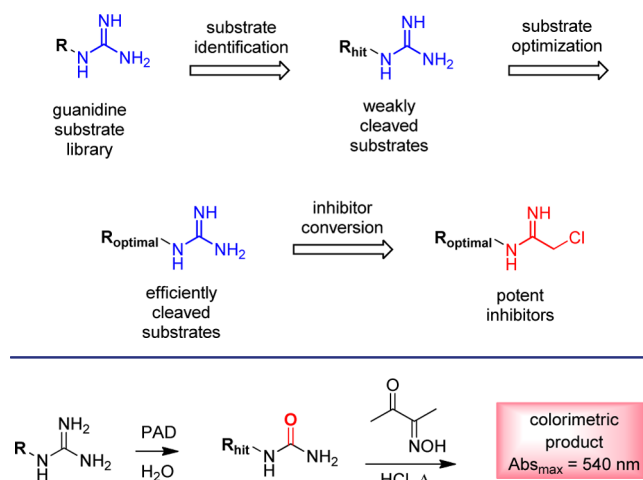Scheme 1. Identification of PAD Inhibitors by SAS

Figure 2. Spectrophotometric detection of substrates.

Table 1. Initial Substrate Hits Against PAD3[a]

	Substrate	Rel. k_{cat}/K_m
1a		1.0 ± 0.1
2a		3.1 ± 0.6
3a		1.0 ± 0.1
4a		3.5 ± 0.4
5a		4.1 ± 0.4

[a]Rel. k_{cat}/K_m was determined using at least four independent measurements at a substrate concentration (1 mM) below the K_m.

Table 2. Optimization of PAD3 Substrate Hit 3a[a,b]

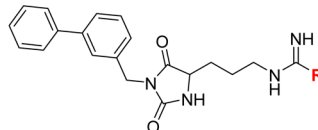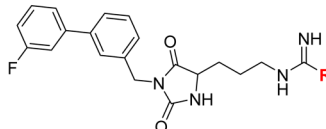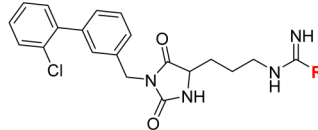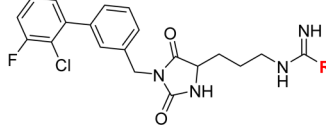| Structure	Substrate (R = NH$_2$) Rel. k_{cat}/K_m	Inhibitor (R = CH$_2$Cl) k_{inact}/K_I (min^{-1}M^{-1})
	3a 1.00 ± 0.1	3b 890 ± 15
	6a 0	ND
	7a 1.90 ± 0.2	7b 900 ± 20
	8a 3.1 ± 0.1	8b 2420 ± 140
	9a 3.90 ± 0.1	9b 2630 ± 290
	10a 10.7 ± 1.1	10b 3330 ± 470
	11a 17.9 ± 1.8	11b 5800 ± 1400
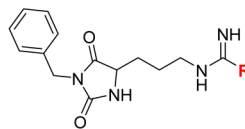
[a]Rel. k_{cat}/K_m was determined using at least four independent measurements at a substrate concentration (1 mM) below the K_m. [b]Unless otherwise noted, k_{inact}/K_I was determined using six concentrations of inhibitor at five time points. $k_{obs} = k_{inact}/K_I$ because $[I] \ll K_i$.[42] The assays were run in duplicate. See Supporting Information for further assay details.

molecular weight guanidines is screened for substrate activity using a colorimetric assay; (2) the identified weakly cleaved guanidine substrates are optimized by analogue synthesis and subsequent screening; and (3) the efficiently cleaved substrates are converted to inhibitors by direct replacement of the guanidine with the chloroacetamidine warhead, a known mechanism-based pharmacophore.[5,39]

Synthesis of Guanidine Substrate Library. More than 200 guanidine substrates were prepared by solution-phase parallel synthesis from primary amine starting materials. A subset of primary amines was selected using 2D extended connectivity analysis from thousands of commercially available amines with molecular weights below 300 Da. Each of the amines was converted into the corresponding guanidines using a one-step guanylation reaction (see Supporting Information). To achieve further substrate diversity, several additional guanidine substrates, containing a variety of heterocyclic scaffolds, were synthesized and included for screening. Subsequent to the identification of hit substrates, analogs of representative hits were also prepared. All guanidine library members were purified by preparative-scale reverse-phase chromatography and assayed for purity using LCMS and NMR spectroscopy.
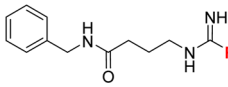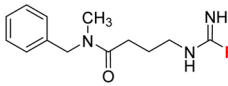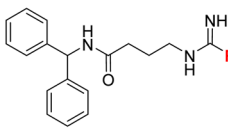
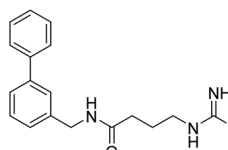## Table 3. Optimization of PAD3 Substrate Hit 4a[a]
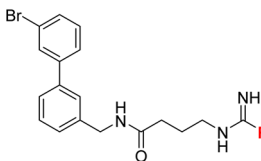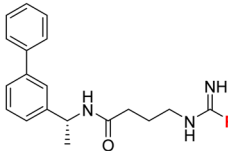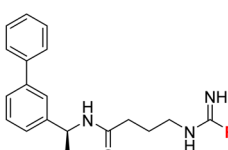
Structure	Substrate (R = NH₂) Rel. k_{cat}/K_m	Inhibitor (R = CH₂Cl) k_{inact}/K_I (min⁻¹M⁻¹)
	4a 3.5 ± 0.4	4b 1620 ± 130
	12a 4.9 ± 0.5	12b 4100 ± 1400
	13a 5.5 ± 0.6	13b 11400 ± 1300
	14a 6.8 ± 0.1	14b 15600 ± 2200
	15a 9.2 ± 0.9	15b 17400 ± 2400

[a]See both footnotes (a and b) from Table 2.

Table 4. Optimization of PAD3 Substrate Hit 5a[a]

Structure	Substrate (R = NH₂) Rel. k_{cat}/K_m	Inhibitor (R = CH₂Cl) k_{inact}/K_I (min⁻¹M⁻¹)
	5a 4.1 ± 0.4	5b 600 ± 180
	16a 0	ND
	17a 11.1 ± 0.2	17b 6300 ± 1100
	18a 14.1 ± 1.4	18b 11000 ± 2100
	19a 15.2 ± 0.4	19b 13220 ± 520
	20a 2.9 ± 0.3	20b 2260 ± 350
	21a 12.8 ± 0.1	21b 13100 ± 1100

[a]See both footnotes (a and b) from Table 2.

Guanidine Library Screening Assay Method. The guanidine library was screened against PAD3 using a colorimetric coupled assay for the detection of urea-containing compounds.[40] Briefly, PAD-mediated substrate turnover results in the formation of an ammonium ion and a urea product. In the presence of strongly acidic conditions and elevated temperatures, reaction of a urea functionality with diacetyl monoxime results in the formation of a chromogenic product that can be detected at 540 nm (Figure 2). This coupled assay was adapted for screening in 96-well plates and spectrophoto-metric plate readers to enable high throughput screening of the guanidine library. To serve as a background control each guanidine substrate was also submitted to the assay conditions without enzyme.

Step 1: Hit Substrate Identification. The guanidine substrate library was initially screened at 1 mM of substrate and 400 nM PAD3. From this screen, multiple distinct substrate classes were identified as weakly cleaved substrate hits. For each of these hits the K_m values were determined to be >10 mM, and thus their relative cleavage efficiency accurately correlates with k_{cat}/K_m (Table 1). Both indole substrate 1a and hydantoin substrates 3a and 4a incorporate known drug pharmacophores with multiple potential sites for diversification. The highest detected relative cleavage efficiency for 5a is also surprising because the amide carbonyl and NH are out of register relative to the placement of these functionalities in physiological Arg-based peptide substrates. Substrate 5a is moreover an attractive starting point for further optimization because it does not contain any chiral centers, and therefore straightforward introduction of alkenes and other conformational constraints

within the alkane chain could be possible. Notably, these types of conformational constraints have proven beneficial in the development of subtype selective histone deacetylase (HDAC) inhibitors.[41] Based on these characteristics, we chose to optimize the hydantoin, benzyl hydantoin, and benzylamide scaffolds. Although benzodiazepine substrate 2a was not chosen for optimization, it represents another possibility for small molecule inhibitor development.

Step 2: Substrate Optimization. *Substrate Evaluation.* The K_m values were determined for representative substrates, and in all cases were >5 mM. Because substrate assays were performed at 1 mM, well below the substrate K_m values, the relative substrate cleavage efficiencies directly correspond to the catalytic efficiencies (k_{cat}/K_m) of the substrates.[28−33]

Hydantoin Substrate Synthesis and Optimization. Hydan-toin derivatives were synthesized by addition of H-Arg(Pbf)-OMe to an isocyanate, followed by cyclization to give hydantoins using basic conditions that also ensure racemization of the methine proton. Racemic rather than enantiomerically pure substrates were synthesized because we established that rapid epimerization at the hydantoin stereocenter occurred at

Table 5. Inhibition of PADs by Hydantoin, Benzyl Hydantoin, and Benzylamide Inhibitors[a]

	k_{inact}/K_I $(min^{-1} M^{-1})$			
compound	PAD1	PAD2	PAD3	PAD4
Cl-amidine	4550 ± 860	520 ± 50	2340 ± 80	1770 ± 470
11b	190 ± 30	1000 ± 10	5800 ± 1400	960 ± 40
14b	360 ± 30	1110 ± 10	15600 ± 2200	1460 ± 60
15b	740 ± 70[b]	1270 ± 70	17400 ± 2400	3380 ± 670
18b	450 ± 120	1130 ± 30[b]	11000 ± 2000	1090 ± 30
19b	540 ± 350[b]	2380 ± 90	13220 ± 520	2170 ± 30[b]

[a]See both footnotes (a and b) from Table 2. [b]For this inhibitor/isozyme combination saturation was achieved, and k_{inact}/K_I was determined by nonlinear regression analysis by fitting the plot of k_{obs} versus [I] for $k_{obs} = k_{inact}[I]/([I] + K_I)$. See Supporting Information for further assay details.

physiological pH and under the assay conditions (see Supporting Information).

Table 2 shows the relative k_{cat}/K_m of select substrates and depicts the optimization of a weakly cleaved initial substrate hit (**3a**) to a substrate that is cleaved 17-fold more efficiently (**11a**). While methylation of the hydantoin at N1 completely abolished activity (**6a**), phenyl substitution of the hydantoin at N3 resulted in a slight improvement in cleavage efficiency and provided a site for further variation (**7a**). Evaluation of several phenyl substituted derivatives resulted in the identification of the 4-methoxyphenyl benzamide analogue **9a**, cleaved with ~2-fold greater cleavage efficiency than the initial hit. Analogues **10a** and **11a** led to significant increases in cleavage efficiency.

Table 3 shows the relative k_{cat}/K_m of selected select substrates for the optimization of substrate hit **4a** to substrate **15a** cleaved almost three times more efficiently. Substrate **12a** with *meta*-phenyl substitution showed a modest increase in k_{cat}/K_m. Further substitution upon this phenyl ring was therefore evaluated. Both *meta*-fluoro (**13a**) and *ortho*-chloro (**14a**) substituents increased substrate activity, and the combination of these substitutions showed a cumulative effect, leading to the most efficiently cleaved substrate in this series, **15a**.

N-Benzyl Amide Substrate Synthesis and Optimization. Derivatives of the *N*-benzyl-amide fragment **5a** were synthesized by a carbodiimide-mediated coupling reaction between *N,N′*-di-Boc-protected γ-aminobutyric acid and various substituted benzylamines (see Supporting Information). As with the phenyl hydantoin series, methyl substitution of the amide NH resulted in a dramatic decrease in substrate activity (**16a**). Several substituents were introduced at the α-benzylic position, with the phenyl group (**17a**) resulting in more than a 2-fold increase in cleavage efficiency as compared to **5a**. Separately, substitutions on the benzyl aromatic ring were investigated, with the phenyl substituted substrate **18a** being cleaved three times more efficiently than the original hit **5a**. Substitutions around the secondary phenyl ring were also tolerated, most notably, **19a** was the most efficiently cleaved substrate in the series. The α-methyl substituted enantiomers **20a** and **21a** were also of interest because they showed strong chiral discrimination with the more active stereoisomer **21a** being cleaved four times more efficiently than its enantiomer **20a**.

Step 3: Conversion of Substrates to Inhibitors. Inhibitors were prepared by replacing the guanidine present in the identified substrates with the known chloroacetamidine irreversible inhibitor pharmacophore. Each substrate with the highest relative k_{cat}/K_m in the three substrate classes was converted to its corresponding inhibitor (Tables 2−4). The optimal *N*-phenyl hydantoin inhibitor **11b** showed a k_{inact}/K_I of 5800 $(min^{-1} M^{-1})$ toward PAD3 (Table 2), the most efficiently cleaved *N*-benzyl amide substrate **19a** resulted in inhibitor **19b**

with a k_{inact}/K_I of 13220 $(min^{-1} M^{-1})$ (Table 4), and the most efficiently cleaved *N*-benzyl hydantoin substrate **15a** was converted to **15b**, which was the most potent inhibitor to be identified with a k_{inact}/K_I of 17400 $(min^{-1} M^{-1})$ (Table 3). These novel, nonpeptidic inhibitors represent distinct structural motifs capable of PAD3 inhibition and serve as useful templates for further optimization.

Additionally, many of the less efficiently cleaved substrates in each series were also converted to inhibitors to enable an assessment of the correlation of substrate cleavage efficiency to inhibitor activity (Tables 2-4). Within each compound series the relative cleavage efficiency and inhibitory potency correlated reasonably well. The most efficiently cleaved substrate also resulted in the most potent inhibitor for each series. However, correlation did not extend across the three series. For example, substrate **11a** (Table 2) was the most efficiently cleaved substrate from all of the compound series, but it did not result in the most potent inhibitor. In fact, substrate **15a**, which corresponded to most potent inhibitor **15b** (Table 3), was ~2-fold less efficiently cleaved than **11a**.

For a related series of substrates and mechanism-based inhibitors, the $log[K_m/k_{cat}]$ often linearly correlates with $log[K_I]$ for the corresponding inhibitors incorporating stable transition-state analogs.[43,44] However, substrate and inhibitor correlation is often more complex. In some cases inhibitors better correlate with the corresponding substrate's ground-state binding (K_m).[36,45] For irreversible inactivators such as those employed in this study, inhibition might correlate better with the k_{cat} term.[46] Unfortunately, because the substrates reported here are not soluble at the high concentrations required to accurately measure K_m, separate k_{cat} and K_m terms could not be determined.

Inhibitor Isozyme Selectivity. The most potent inhibitor in each compound series was evaluated for isozyme selectivity (Table 5). Inhibitors **11b**, **15b**, and **19b** each were highly selective over PAD1 but showed more modest 5−6-fold selectivity over PADs 2 and 4. However, two of the more potent inhibitors in the *N*-benzyl hydantoin and *N*-benzyl amide series, **14b** and **18b**, respectively, showed ≥10-fold selectivity not only over PAD1 but also over PADs 2 and 4.[47] Given the potency and selectivity observed for **14b** and **18b**, these two structures are particularly promising for biological studies as well as for further inhibitor development.

■ CONCLUSION

Low molecular weight, nonpeptidic and selective inhibitors of the PAD isozymes have the potential to be powerful pharmacological tools for evaluating the roles of PADs in a number of disease states. This report describes the discovery of PAD3 selective small molecule inhibitors. We have successfully

implemented a substrate-based fragment discovery method for identifying PAD inhibitors by screening a library of guanidines to identify substrates, optimizing substrate structure for cleavage efficiency and then conversion to inhibitors by replacement of the guanidine by the chloroacetamidine inhibitor pharmacophore. This method enabled the rapid identification of three distinct classes of small molecule inhibitors. Inhibitor **14b**, with a k_{inact}/K_I of 15,600 toward PAD3 had the optimal combination of potency and selectivity.

■ ASSOCIATED CONTENT

ⓢ Supporting Information

Complete experimental procedures and characterization data for all compounds described as well as k_{inact}/K_I data for all inhibitors. This material is available free of charge via the Internet at http://pubs.acs.org.

■ AUTHOR INFORMATION

Corresponding Author

*jonathan.ellman@yale.edu

Present Addresses

†RA Pharmaceuticals, One Kendall Square #B7202, Cambridge, MA, 02139

‡Melinta Therapeutics, 300 George Street, New Haven, CT 06511−663

Notes

The authors declare no competing financial interest.

■ ACKNOWLEDGMENTS

■ REFERENCES

(1) Vossenaar, E. R.; Zendman, A. J. W.; van Venrooij, W. J.; Pruijn, G. J. M. *Bioessays* **2003**, *25*, 1106.

(2) Bicker, K. L.; Thompson, P. R. *Biopolymers* **2013**, *99*, 155.

(3) Jones, J. E.; Causey, C. P.; Knuckley, B.; Slack-Noyes, J. L.; Thompson, P. R. *Curr. Opin. Drug Discovery Dev.* **2009**, *12*, 616.

(4) Knuckley, B.; Causey, C. P.; Jones, J. E.; Bhatia, M.; Dreyton, C. J.; Osborne, T. C.; Takahara, H.; Thompson, P. R. *Biochemistry* **2010**, *49*, 4852.

(5) Luo, Y.; Arita, K.; Bhatia, M.; Knuckley, B.; Lee, Y.-H.; Stallcup, M. R.; Sato, M.; Thompson, P. R. *Biochemistry* **2006**, *45*, 11727.

(6) Arita, K.; Hashimoto, H.; Shimizu, T.; Nakashima, K.; Yamada, M.; Sato, M. *Nat. Struct. Mol. Biol.* **2004**, *11*, 777.

(7) Kearney, P. L.; Bhatia, M.; Jones, N. G.; Yuan, L.; Glascock, M. C.; Catchings, K. L.; Yamada, M.; Thompson, P. R. *Biochemistry* **2005**, *44*, 10570.

(8) Ishida-Yamamoto, A.; Senshu, T.; Takahashi, H.; Akiyama, K.; Nomura, K.; Iizuka, H. *J. Invest. Dermatol.* **2000**, *114*, 701.

(9) Raijmakers, R.; Vogelzangs, J.; Raats, J.; Panzenbeck, M.; Corby, M.; Jiang, H. P.; Thibodeau, M.; Haynes, N.; Van Venrooij, W. J.; Pruijn, G. J. M.; Werneburg, B. *J. Comp. Neurol.* **2006**, *498*, 217.

(10) Wood, D. D.; Ackerley, C. A.; van den Brand, B.; Zhang, L.; Raijmakers, R.; Mastronardi, F. G.; Moscarello, M. A. *Lab. Invest.* **2008**, *88*, 354.

(11) Musse, A. A.; Li, Z.; Ackerley, C. A.; Bienzle, D.; Lei, H.; Poma, R.; Harauz, G.; Moscarello, M. A.; Mastronardi, F. G. *Dis. Model. Mech.* **2008**, *1*, 229.

(12) Moscarello, M. A.; Wood, D. D.; Ackerley, C.; Boulias, C. *J. Clin. Invest.* **1994**, *94*, 146.

(13) (I) For the link between PAD4 and rhuematoid arthritis, see: (a) Kinloch, A.; Lundberg, K.; Wait, R.; Wegner, N.; Lim, N. H.; Zendman, A. J. W.; Saxne, T.; Malmstrom, V.; Venables, P. J. *Arthritis Rheum.* **2008**, *58*, 2287. (b) Masson-Bessiere, C.; Sebbag, M.; Girbal-Neuhauser, E.; Nogueira, L.; Vincent, C.; Senshu, T.; Serre, G. *J. Immunol.* **2001**, *166*, 4177. (c) Schellekens, G. A.; de Jong, B. A. W.; van den Hoogen, F. H. J.; van de Putte, L. B. A.; van Venrooij, W. J. *J. Clin. Invest.* **1998**, *101*, 273. (II) For the link between PAD4 and ulcerative colitis, see: (d) Chen, C.; Isomoto, H.; Narumi, Y.; Sato, K.; Oishi, Y.; Kobayashi, T.; Yanagihara, K.; Mizuta, Y.; Kohno, S.; Tsukamoto, K. *Clin. Immunol.* **2008**, *126*, 165. (III) For the link between PADs and lupus, see: (e) Knight, J. S.; Zhao, W.; Luo, W.; Subramanian, V.; O'Dell, A. A.; Yalavarthi, S.; Hodgin; Eitzman, D.; Thompson, P. R.; Kaplan, M. *J. Clin. Invest.* **2013**, *123*, 2981.

(14) Monahan, S.; Cherrington, B. D.; Horibata, S.; McElwee, J. L.; Thompson, P. R.; Coonrod, S. A. *Biochem. Res. Int.* **2012**, *2012*, 11.

(15) Lange, S.; Gogel, S.; Leung, K. Y.; Vernay, B.; Nicholas, A. P.; Causey, C. P.; Thompson, P. R.; Greene, N. D. E.; Ferretti, P. *Dev. Biol.* **2011**, *355*, 205.

(16) The inhibitor values reported here were performed in our lab with 0.1% of Triton-X in the assay buffer to prevent micelle formation and with 5% of DMSO, which was needed to solubilize some of the inhibitors to determine isozyme selectivitry. For Cl-amidine, the Thompson lab performed assays without Triton-X or DMSO and observed a different k_{inact}/K_i values with the largest difference for PAD1. We established that while the presence of Triton-X had minimal affect on a k_{inact}/K_i values, as little as 1% DMSO caused a pronounced reduction in Cl-amidine inhibitor potency for PAD1.

(17) An analog of Cl-amidine with comparable enzyme inhibitory activity and good cell and animal efficacy has recently been reported: Knight, J. S.; Subramanian, V.; O'Dell, A. A.; Yalavarthi, S.; Zhao, W.; Smith, C. K.; Hodgin, J. B.; Thompson, P. R.; Kaplan, M. J. *Ann. Rheum. Dis.* [Online early access]. DOI: 10.1136/annrheumdis-2014-205365 Published Online: Aug 7, **2014**.

(18) Willis, V.; Gizinski, A. M.; Banda, N. K.; Causey, C. P.; Knuckley, B.; Cordova, K. N.; Luo, Y. A.; Levitt, B.; Glogowska, M.; Chandra, P.; Kulik, L.; Robinson, W. H.; Arend, W. P.; Thompson, P. R.; Holers, V. M. *J. Immunol.* **2011**, *186*, 4396.

(19) Causey, C. P.; Jones, J. E.; Slack, J. L.; Kamei, D.; Jones, L. E.; Subramanian, V.; Knuckley, B.; Ebrahimi, P.; Chumanevich, A. A.; Luo, Y.; Hashimoto, H.; Sato, M.; Hofseth, L. J.; Thompson, P. R. *J. Med. Chem.* **2011**, *54*, 6919.

(20) F4-amidine and Cl4-amidine were previously reported by the Thompson group as inhibitors that show PAD3 selectivity relative to PAD1 and PAD4, although no inhibitory data was provided for PAD2 (see reference 4). An exact IC_{50} value of 65 μM for PAD3 was reported for F4-amidine. The approximate IC_{50} values for F4-amidine for PAD1 and PAD4 as provided in the chart in Figure 6A were ∼250 μM and ∼625 μM, respectively.

(21) Knuckley, B.; Jones, J. E.; Bachovchin, D. A.; Slack, J.; Causey, C. P.; Brown, S. J.; Rosen, H.; Cravatt, B. F.; Thompson, P. R. *Chem. Commun.* **2010**, *46*, 7175.

(22) Knuckley, B.; Luo, Y.; Thompson, P. R. *Bioorg. Med. Chem.* **2008**, *16*, 739.

(23) Slack, J. L.; Causey, C. P.; Luo, Y.; Thompson, P. R. *ACS Chem. Biol.* **2011**, *6*, 466.

(24) Wood, W. J. L.; Patterson, A. W.; Tsuruoka, H.; Jain, R. K.; Ellman, J. A. *J. Am. Chem. Soc.* **2005**, *127*, 15521.

(25) For the potential for nonadditivity in substrate fragments, see: Barelier, S.; Cummings, J. A.; Rauwerdink, A. M.; Hitchcock, D. S.; Farelli, J. D.; Almo, S. C.; Raushel, F. M.; Allen, K. N.; Shoichet, B. K. *J. Am. Chem. Soc.* **2014**, *136*, 7374.

(26) McGovern, S. L.; Caselli, E.; Grigorieff, N.; Shoichet, B. K. *J. Med. Chem.* **2002**, *45*, 1712.

(27) Feng, B. Y.; Shoichet, B. K. *Nat. Protoc.* **2006**, *1*, 550.

(28) Brak, K.; Doyle, P. S.; McKerrow, J. H.; Ellman, J. A. *J. Am. Chem. Soc.* **2008**, *130*, 6404.

(29) Leyva, M. J.; DeGiacomo, F.; Kaltenbach, L. S.; Holcomb, J.; Zhang, N.; Gafni, J.; Park, H.; Lo, D. C.; Salvesen, G. S.; Ellerby, L. M.; Ellman, J. A. *Chem. Biol.* **2010**, *17*, 1189.

(30) Patterson, A. W.; Wood, W. J. L.; Ellman, J. A. *Nat. Protoc.* **2007**, *2*, 424.

(31) Patterson, A. W.; Wood, W. J. L.; Hornsby, M.; Lesley, S.; Spraggon, G.; Ellman, J. A. *J. Med. Chem.* **2006**, *49*, 6298.

(32) Salisbury, C. M.; Ellman, J. A. *ChemBioChem* **2006**, *7*, 1034.

(33) Inagaki, H.; Tsuruoka, H.; Hornsby, M.; Lesley, S. A.; Spraggon, G.; Ellman, J. A. *J. Med. Chem.* **2007**, *50*, 2693.

(34) Baguley, T. D.; Xu, H.-C.; Chatterjee, M.; Nairn, A. C.; Lombroso, P. J.; Ellman, J. A. *J. Med. Chem.* **2013**, *56*, 7636.

(35) Rawls, K. A.; Therese Lang, P.; Takeuchi, J.; Imamura, S.; Baguley, T. D.; Grundner, C.; Alber, T.; Ellman, J. A. *Bioorg. Med. Chem. Lett.* **2009**, *19*, 6851.

(36) Soellner, M. B.; Rawls, K. A.; Grundner, C.; Alber, T.; Ellman, J. A. *J. Am. Chem. Soc.* **2007**, *129*, 9613.

(37) Breen, M. E.; Steffey, M. E.; Lachacz, E. J.; Kwarcinski, F. E.; Fox, C. C.; Soellner, M. B. *Angew. Chem., Int. Ed.* **2014**, *53*, 7010.

(38) Chapelat, J.; Berst, F.; Marzinzik, A. L.; Moebitz, H.; Drueckes, P.; Trappe, J.; Fabbro, D.; Seebach, D. *Eur. J. Med. Chem.* **2012**, *57*, 1.

(39) (a) Knuckley, B.; Causey, C. P.; Pellechia, P. J.; Cook, P. F.; Thompson, P. R. *ChemBioChem.* **2010**, *11*, 161. (b) Knuckley, B.; Bhatia, M.; Thompson, P. R. *Biochemistry* **2007**, *46*, 6578.

(40) Knipp, M.; Vašák, M. *Anal. Biochem.* **2000**, *286*, 257.

(41) Marks, P. A. *Exp. Opin. Investig. Drugs* **2010**, *19*, 1049.

(42) To determine k_{inact}/K_I, plots of k_{obs} vs inhibitor concentration were fit to a Kitz−Wilson model: Kitz, R.; Wilson, I. B. *J. Biol. Chem.* **1962**, *237*, 3245. The inhibitor concentrations used in the reported assays corresponded to $[I] \ll K_I$. The slope of the resulting line therefore equals k_{inact}/K_I.

(43) For a review on the correlation between kinetic parameters of substrate turnover and enzyme inhibition, see: (a) Mader, M. M.; Bartlett, P. A. *Chem. Rev.* **1997**, *97*, 1281. For an initial description of transition-state theory and the relationship of substrate and corresponding inhibitor families, see: (b) Lienhard, G. E. *Science* **1973**, *180*, 149. (c) Wolfenden, R. *Annu. Rev. Biophys. Bioeng.* **1976**, *5*, 271. For early experiments characterizing the correlation of peptidic substrates families and their corresponding peptidic inhibitors, see: (d) Thompson, R. C. *Biochemistry* **1973**, *12*, 47. (e) Bartlett, P. A.; Marlowe, C. K. *Biochemistry* **1983**, *22*, 4618. (f) Bartlett, P. A.; Otake, A. *J. Org. Chem.* **1995**, *60*, 3107.

(44) Frick, J.; Wolfenden, R. *Design of Enzyme Inhibitors as Drugs*; Oxford University Press: New York, 1989.

(45) Drag, M.; Bogyo, M.; Ellman, J. A.; Salvesen, G. S. *J. Biol. Chem.* **2010**, *285*, 3310.

(46) Rando, R. R. *Science* **1974**, *185*, 320.

(47) The corresponding IC_{50} values for the most selective inhibitors reported in this study are: 120, 27.5, 4.5, and 30.5 μM for **14b** against PADs 1, 2, 3, and 4, respectively, and 81, 46, 5.8 and 39 μM for **18b** against PADs 1, 2, 3, and 4, respectively. These IC_{50} values compare favorably with the IC_{50} data for F4-amidine (see ref 20).